

Organic & Biomolecular Chemistry

Accepted Manuscript



This article can be cited before page numbers have been issued, to do this please use: R. Alam, A. S. M. Islam, M. Sasmal, A. Katarkar and A. Mahammad, *Org. Biomol. Chem.*, 2018, DOI: 10.1039/C8OB00822A.



This is an Accepted Manuscript, which has been through the Royal Society of Chemistry peer review process and has been accepted for publication.

Accepted Manuscripts are published online shortly after acceptance, before technical editing, formatting and proof reading. Using this free service, authors can make their results available to the community, in citable form, before we publish the edited article. We will replace this Accepted Manuscript with the edited and formatted Advance Article as soon as it is available.

You can find more information about Accepted Manuscripts in the [author guidelines](#).

Please note that technical editing may introduce minor changes to the text and/or graphics, which may alter content. The journal's standard [Terms & Conditions](#) and the ethical guidelines, outlined in our [author and reviewer resource centre](#), still apply. In no event shall the Royal Society of Chemistry be held responsible for any errors or omissions in this Accepted Manuscript or any consequences arising from the use of any information it contains.



Journal Name

ARTICLE

Rhodamine-based turn-on nitric oxide sensor in aqueous medium with endogenous cell imaging: an unusual formation of nitrosohydroxylamine

Received 00th January 20xx,
Accepted 00th January 20xx

DOI: 10.1039/x0xx00000x

www.rsc.org/

Rabiul Alam^a, Abu Saleh Musha Islam^a, Mihir Sasmal^a, Atul Katarkar^b and Mahammad Ali^{a,*}

A newsensor (**L**³) based on RhodamineB-en(**2**) and 2-(Pyridin-2-ylmethoxy)benzaldehyde (**1**) has been developed for highly sensitive and selective recognition of NO in purely aqueous medium where the reaction of NO with the fluorophore leads to an unusual formation of nitrosohydroxylamine with the selective opening of spirolactam ring over different cations, anions, amino-acids and other biological species with prominent enhancement in absorption and emission intensities. A large enhancement of fluorescence intensity for NO (11 fold) was observed upon addition of 3 equivalents of NO into the sensor in aqueous HEPES buffer (20 mM) at pH 7.20, $\mu = 0.05$ M NaCl with a naked eye detection. The corresponding K_f value was evaluated to be $(7.55 \pm 2.04) \times 10^4 \text{ M}^{-1}$ from fluorescence titration plot. Quantum yields of **L**³ and [**L**³ + NO] compound are found to be 0.07 and 0.77 respectively using Rhodamine-6G as standard. LOD for NO was determined by 3σ method and found to be 83.4 nM. **L**³ sensor is low-cytotoxic, cell permeable and suitable for *in vitro* NO sensing. The *in vivo* compatibility of the sensor was also checked on Zebra fish.

Introduction

Nitric oxide (NO), a gaseous, paramagnetic and highly reactive radical molecule, plays various physiological and pathological roles through rapid reaction with other radicals or metalloproteins in the organisms. NO is an important signaling molecule involved in the regulation of a wide range of biological processes such as blood-pressure regulation of the cardiovascular system, antitumor activity of the immune systems and the neurotransmission, vasodilatation and hormone secretion in living bodies¹⁻⁵ and capturing great attention of biologists, chemists, and medical researchers. Furthermore, NO is an effective sacrificial antioxidant in the free radical induced lipid oxidation and a promising anticancer agent.^{6,7} Although, a large variety of quantification techniques have been developed for NO sensing, fluorescence techniques attract considerable attention owing to their sensitivity and high spatiotemporal resolution when combined with microscopy.^{8,9}

The chemistry of NO in aqueous solution is extensively different

from endogenously synthesized NO from the fact that the later has a very short half-life ($t_{1/2} \leq 5$ sec)^{10,11} compared to that in pure aqueous solution of comparable concentration (0.01-10 μM , $t_{1/2} \leq 500$ sec).¹² Thus, in intact cells, tissues, and whole animals NO is highly labile and rapidly metabolized (oxidized) to both NO_2^- and NO_3^- .

A number of fluorescent NO sensors have been reported to date¹³⁻³⁶ still the research on nitric oxide sensors is in its infant stage. The most common approach for NO detection includes the use of *o*-diamino aromatics under aerobic conditions (Scheme 1A).¹⁷ These species react with NO^+ , or N_2O_3 , to furnish fluorescent triazole derivatives.^{13,14,16-18} Turn-on fluorescence signals are achieved through inhibition of photoinduced electron transfer (PET). Very recently there are reports on NO sensing by rhodamine based fluorophores where the fluorescence is restored when the ring is opened in the presence of NO (Scheme 1B).²² Another approach of a turn-on nonfluorescent sensor for NO through oxidative deamination of an aromatic primary monoamine has also been reported (Scheme 1C).³⁷ Another method is developed where N-nitrosation leading to the formation of diazo ring occurs. (Scheme 1D)²⁷

In the present report, we are going to disclose, for the first time, a RhodamineB-en (en = ethylenediamine) and 2-(Pyridin-2-ylmethoxy)benzaldehyde conjugated Schiff base (Scheme 2) as a highly sensitive and selective fluorescent chemosensor for NO in purely aqueous medium with an unusual formation of

^a Department of Chemistry, Jadavpur University, 188 Raja S. C. Mallick Road, Jadavpur, Kolkata 700 032, India. E-mail: m_ali2062@yahoo.com Address here.

^b Department of Molecular & Human Genetics Division, CSIR-Indian Institute of Chemical Biology, 4 Raja S. C. Mallick Road, Kolkata-700032, India

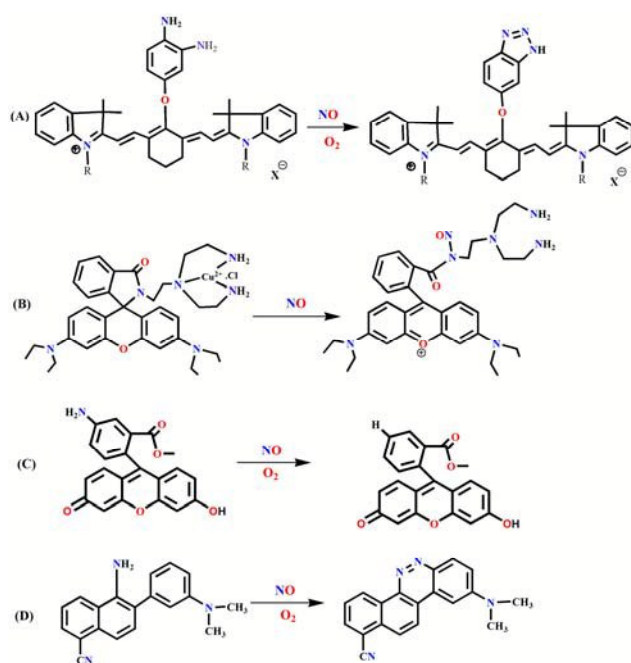
† Footnotes relating to the title and/or authors should appear here.

Electronic Supplementary Information (ESI) available: Information on the synthesis and corresponding characterization data for compound **L**³, ¹H NMR spectra, ¹³C NMR spectra. This material is available free of charge via the Internet at <http://pubs.acs.org>. See DOI: 10.1039/x0xx00000x

ARTICLE

Journal Name

nitrosohydroxylamine along with the opening of spirolactam ring resulting a change in both absorption and fluorescence properties of the sensor. **L**³ is a simple Rhodamine based sensor with a large turn-on fluorescence property (11 fold) along with the very low LOD (83.4 nM) suitable for *in-vivo* monitoring of NO. It has been observed that **L**³ can trap NO mostly in the cytoplasmic compartment. The *in vivo* compatibility of the probe was also checked on live Zebra fish. The sensor is highly selective in pure aqueous medium towards NO, in the presence of different anions, amino-acids and other biological anions with prominent enhancement in absorption and emission intensities. **L**³ molecule is a superior NO sensor based on the unusual formation of nitrosohydroxylamine and as a model for selective drug delivery to the cancer cells where NO concentration is believed to be higher. The nitrosohydroxylamine derivative, Rh-en-ONO, may be useful as a nitrovasodilator drug and may be a subject of elaborative studies.



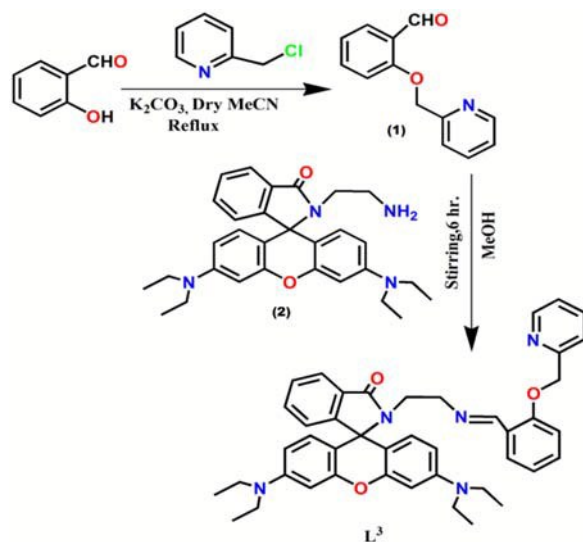
Scheme 1: Typical mechanism for NO detection.

Experimental Section

Materials and Instruments

Elemental analyses were carried out using a Perkin–Elmer 240 elemental analyzer. Infrared spectra (400–4000 cm^{-1}) were recorded in liquid state on a Nicolet Magna IR 750 series-II FTIR spectrometer. ^1H NMR spectra were recorded in CDCl_3 and CD_3CN solutions on a Bruker 300 MHz (AVI, 300) NMR spectrometer. Chemical shifts are expressed in parts per million (ppm, δ) and are referenced to tetramethylsilane ($\delta = 0$) as an internal standard. Signal description: s = singlet, d =

doublet, t = triplet, m = multiplet, dd = doublet of doublets, q = quartet. ^{13}C NMR spectra were recorded in CD_3CN solutions with complete proton decoupling. ESI-MS⁺ (m/z) of the ligand and products of reaction with NO were recorded on a Waters' HRMS spectrometer (Model: XEVO G2QToF). UV-Vis spectra were recorded on an Agilent diode-array spectrophotometer (Model, Agilent 8453). Steady-state fluorescence measurements were performed with a PTI QM-40 spectrofluorometer. pH of the reaction solutions were recorded in a Digital pH meter (Model: Systronics 335, India) in the pH range 2–12 which was prior calibrated using buffers of pH 4, 7 and 10.



Scheme 2: Synthetic route of **L**³

All solvents used for synthesis were of reagent-grade (Merck) unless otherwise mentioned. For spectroscopic (UV-Vis and fluorescence) studies double-distilled water was used. Rhodamine-B and salts such as the perchlorates of Na^+ , Fe^{2+} , Co^{2+} , Ni^{2+} , Zn^{2+} , Pb^{2+} , Cd^{2+} , Hg^{2+} , Cu^{2+} and $\text{Al}(\text{NO}_3)_3 \cdot 9\text{H}_2\text{O}$, $\text{CrCl}_3 \cdot 6\text{H}_2\text{O}$, $\text{Fe}(\text{NO}_3)_3 \cdot 9\text{H}_2\text{O}$ and sodium salts of anions like SCN^- , NO_3^- , N_3^- , Cl^- , Br^- , F^- , HCO_3^- , ClO_4^- , H_2O_2 , OAc^- , $\text{S}_2\text{O}_3^{2-}$, CN^- etc were purchased from Sigma–Aldrich and Merck and used as received. All other compounds were purchased from commercial sources and used as received.

Preparation 2-(Pyridin-2-ylmethoxy) benzaldehyde (1)

Salicylaldehyde (10 mmol, 1.23 g) and K_2CO_3 (18 mmol, 2.52 g) were added to dry MeCN (60 mL), and the mixture was heated at reflux for 40 min. 2-picolyl chloride (11.5 mmol, 1.89 g) and a catalytic amount of KI (0.15 g) was then added to the above reaction mixture, which was heated at reflux for a further 12 h. Then the mixture was cooled and filtered. The filtrate was evaporated to one third of its initial volume and diluted with water (40 mL). Then the pH of the solution was adjusted to 4 by the addition of 1 mL HCl and extracted with dichloromethane (DCM; 2 x 40 mL). The pH of the

aqueous solution was then adjusted to 8 by the addition of 4M Na₂CO₃ solution and extracted with DCM (3 x 40mL). Then the combined organic phase after drying over anhydrous Na₂SO₄ was evaporated to dryness under reduced pressure to give a pale yellow solid residue. The crude solid product was recrystallized from MeOH/DCM (8:2, v/v) to give the desired product as an off-white crystalline solid (66% yield), M.P: 69.4 °C. ¹H NMR (CDCl₃): δ = 10.62 (s, 1H), 8.61 (dd, 1H), 7.86 (dd, 1H), 7.77(td, 1H), 7.53(m, 2H), 7.26 (dd, 1H), 7.05 (m, 2H), 5.33 (s, 2H) ppm (Fig. S1a). ¹³C NMR (CDCl₃): δ = 189.53, 160.59, 156.32, 149.35, 137.04, 135.98, 128.85, 126.21, 125.16, 122.96, 121.26, 110.53, 71.10 ppm (Fig. S2a). MS (ES⁺): *m/z* = 214.07 [(1)+H]⁺ (Fig. S3a) IR: 1690(CHO), 1253 (aliphatic C–O) cm⁻¹ (Fig. S4a). C₁₃H₁₁NO₂ (213.23): calculated. C, 73.23; H, 5.20; N, 6.57; found C, 73.24; H, 5.19; N, 6.58.

Preparation of Rhodamine B-ethylenediamine (2)

RhodamineB–ethylenediamine conjugate was prepared according to a literature method.³⁸

Preparation of the sensor L³

(1)(1.1 mmol, 0.234 g) was dissolved in MeOH (10 mL). Then this solution was added drop wise over 30 min to a methanolic solution (30 mL) of (2) (1 mmol, 0.484 g) under hot (50–60 °C) conditions. The resulting reaction mixture was stirred for 6 h at room temperature. An off-white precipitate was formed, which was collected by filtration. The residue was washed thoroughly with cold methanol and L³ was obtained in pure form. Yield: 84%. ¹H NMR (CDCl₃): δ = 8.70 (s, 1 H), 8.59(d, 1 H), 7.88 (m, 1H), 7.85 (d, 1H), 7.72(d, 1H), 7.49(d, 1H), 7.42(m, 2H), 7.29(d, 1H), 7.22(d, 1H), 7.08 (d, 1H), 6.93(d, 1H), 6.87(d, 1H), 6.48(s, 1H), 6.45(s, 1H), 6.38(s, 2H), 6.24 (dd, 2H), 5.23(s, 2H) 3.48 (t, 2H), 3.40 (t, 2H), 3.31(q, 8H), 1.41 (t, 12 H) ppm (Fig. S1b). ¹³C NMR (CD₃CN):167.63, 157.53, 156.89, 153.83, 153.31, 149.25, 148.93, 136.93, 132.53, 131.84, 131.14, 128.79, 127.27, 125.03, 123.44, 122.88, 121.50, 121.05, 117.34, 112.10, 108.25, 105.58, 97.40, 71.03, 64.62, 58.89, 43.99, 40.97, 11.80 ppm (Fig. S2b). MS (ES⁺): *m/z* = 680.39 [L³ + H]⁺ (Fig. S3b). IR: 1684 cm⁻¹ (C=O), 1634 cm⁻¹ (C=N) (Fig. S4b). C₄₃H₄₅N₅O₃ (679.85): calculated. C, 75.97; H, 6.67; N, 10.30; found C, 75.94; H, 6.68; N, 10.31.

Computational Details

L³ was fully optimized using Gaussian 09W software package.³⁹ The B3LYP functional has been adopted with 6-31G as basis set for all the atoms (C, H, N and O). The global minima of all these species were confirmed by the positive vibrational frequencies. Time dependent density functional theory (TDDFT)^{40,41} with B3LYP density functional associated with the conductor-like polarizable continuum model (CPCM)⁴²⁻⁴⁴ were applied to study the low-lying excited states of the ligand and the product in H₂O using the optimized geometry of the ground (S₀) state. The vertical excitation energies of the lowest 20 singlet states are also computed here.

Cell culture.

HepG2 cell line (NCL, Pune, India) were used in the present study. HepG2 cells were maintained in conditioned media DMEM (Gibco BRL) supplemented with 10% FBS (Gibco, BRL) and antibiotics (penicillin-100 µg/mL; streptomycin-50 µg/mL) at 37°C (5% CO₂ incubator).

Cell Cytotoxicity Assay

Cell viability assay of ligand L³ was performed by using MTT as explained elsewhere.⁴⁵

Griess Assay

HepG2 cells were seeded at a density of 1×10³ cells/well in a 96-well plate, and were incubated for 12 h. 1µM/mL sodium nitroprusside (SNP), 10 µM/mL L-arginine (L-Arg) and 0.5 µg/mL LPS+ 5ng/mL IFN-γ were treated to the cells compared with control and selective iNOS inhibitor, S-Methylisothiourea Sulfate (SMT) (10 µg/mL). After 24 h, the level of NO production was evaluated using the Griess Reagent system according to the manufacturer's instructions. Briefly, 50 µL of each cell culture medium were added to a 96-well plate in triplicate. 50 µL of sulfanilamide solution were dispensed to each sample well, and the plate was incubated at 25 °C in the dark. After 10 min, 50 µL of N-1-naphthylethylenediamine dihydrochloride (NED) solution was added to the mixture and the plate was incubated at 25 °C for another 10 min in the dark. The production of NO for each sample well was measured at 523 nm (EMax Precision MicroPlate Reader, Molecular Devices, USA).

iNOS Expression Study

We verified the iNOS mediated increase in NO production in the SNP and (L-Arg + LPS + IFN-γ) treated HepG2 cells. We examined the expression of iNOS at mRNA and protein in total cell extracts after treating the HepG2 cells with SNP or (L-Arg and LPS + IFN-γ) for 24h and compared to control and SMT. 1×10³ cells were seeded on 60 mm culture dish and incubated for 12h, after incubation cells were treated with 1µM/mL SNP or (10 µM L-Arg and 0.5 µg/mL LPS + 5ng/mL IFN-γ) and iNOS inhibitor SMT (10 µg/mL) for 24h. The cells were harvested, and total RNA was prepared by the TRIzol method (invitrogen). The iNOS mRNA level in different settings was measured by semi-Quantitative RT-PCR by using iNOSForward primer 5'-TCC CGA AGT TCT CAA GGC AC-3' reverse primer 5'-TGG CTT TAC AAA GCA GGT CAC-3'. GAPDH was used as an internal control and its level was measured by forward primer 5'- TTC GAC AGT CAG CCG CATC-3' and Reverse primer 5'- GGC GCC CAA TAC GAC CAA AT-3'. Cytosolic extract preparation and Western blot analysis of iNOS were performed with rabbit anti-human iNOS antibodies (Santa Cruz Biotechnology, CA). 50 µg protein from total cell extracts were estimated by using Bradford reagent (Sigma-Aldrich), which were loaded onto 10% sodium dodecyl sulfate-polyacrylamide gel electrophoresis gels and examined by Western

ARTICLE

Journal Name

blot analysis. Incubation with a specific anti-iNOS rabbit polyclonal antibody (diluted 1:1,000) and anti- β -actin mouse monoclonal antibody (diluted 1:1000) was performed for overnight at 4°C. The blots were then incubated with a secondary antibody, horseradish peroxidase-linked anti-rabbit (diluted 1:2,500) or anti-mouse (diluted 1:10,000) immunoglobulin, for 2 h at room temperature. The blots were detected by using DAB method. Densitometry was performed using Image-J Software (NIH, USA). The β -Actin was used as internal control.

Cell imaging study by fluorescence microscope

1×10^4 HepG2 cells were cultured and incubated in 35x10 mm culture dish over the coverslip for 24h at 37°C in the media (DMEM, 10% FBS). Then HepG2 cells were treated with $1 \mu\text{M}/\text{mL}$ SNP or ($10 \mu\text{M}/\text{mL}$ L-Arg, $0.5 \mu\text{g}/\text{mL}$ LPS+ $5 \text{ng}/\text{mL}$ IFN- γ), also along with $10 \mu\text{g}/\text{mL}$ SMT and control cells kept untreated for 24 h at 37°C followed by treated with $10 \mu\text{M}$ of L^3 for 30 min at 37°C. This all procedure was performed into the Media (DMEM, 10% FBS) itself and to visualize live cells on coverslip it was washed with PBS before mounting on microscope to visualize the cells. Bright field and fluorescence images of HepG2 cells were taken by fluorescence microscope (Leica DM3000, Germany) with an objective lens of 40X magnification. Owing to L^3 has cell permeability and rapid fluorescence response to NO, L^3 was further tested for real time monitoring of NO. During this process or during treatments cells were not fixed with paraformaldehyde or formaldehyde or any fixing reagents etc.

Zebra fish imaging studies

As living cells and organ needs NO for the physiological processing, signaling, homeostasis and organ development, living tissues have been found to continuously release NO. Despite of this, Zebrafish (*Danio rerio*) are progressively cast-off in research and has established as a valuable animal model for drug discovery and to screen bioactive compounds.⁴⁶ Several studies had used zebrafish as animal model to check the exogenous effect of NO in tonus develops, inflammatory events and control of breathing.^{47,48} To take an advantage of this method we used zebrafish as model to trap SNP induced NO. Adult and healthy wild type zebrafish (4-5-week-old zebrafish) of both sexes were obtained from a local fish supplier (average weight $0.6870.05 \text{ g}$ and average length $3.9570.07 \text{ cm}$) and kept in aquaria. The fish were fed twice a day with commercial food (Optimum, Thailand) and water was changed daily to discard metabolic wastes. Zebrafishes were maintained at controlled environment (25°C , 12h:12h light: dark) were incubate without and with $0.5 \mu\text{M}$ SNP for 60 min, washed with vehicle, incubated with $20 \mu\text{M}$ of L^3 for 45 min and further allowed for washing in L^3 free vehicle. The images were captured in objective lens of 40X magnification.

Results and discussion

As depicted in Scheme 2, receptor L^3 was synthesized from the reaction of rhodamine-B with ethylenediamine followed by Schiff base condensation with O-pyridyl-salicylaldehyde (1) which was well characterized by ^1H NMR (Fig.S1), ^{13}C NMR (Fig. S2), HRMS (Fig.S3) and IR (Fig.S4). The receptor L^3 was found to be highly sensitive and selective fluorogenic sensor for NO in aqueous media. The sensor is not freely soluble in aqueous medium. For both UV-Vis and fluorescence titrations, a $10 \text{ mL } 1.0 \times 10^{-3} \text{ M}$ stock solutions of L^3 was prepared by dissolving it in few drops of MeCN and then volume was adjusted with HEPES buffer at pH 7.20, $\mu = 0.05 \text{ M}$ NaCl. 2.5 mL buffer solution was pipetted out into a cuvette to which $50 \mu\text{L}$ of the sensor was added to get $20 \mu\text{M}$ L^3 and NO were added incrementally ($0 - 60 \mu\text{M}$) in a regular interval.

UV-Vis absorption studies

In order to determine the equilibrium constant for the reaction between L^3 and NO a UV-Vis titration with the fixed concentration of L^3 ($20 \mu\text{M}$) and variable concentration of NO ($0 - 80.0 \mu\text{M}$) at 25°C in aqueous HEPES buffer (20 mM) at pH 7.20, $\mu = 0.05 \text{ M}$ NaCl was carried out. It was revealed that there is a gradual development of a new absorption band at around 561 nm (Fig. 1a) with the addition of NO. A plot of Absorbance vs. $[\text{NO}]$ yield a non-linear curve of decreasing slope (Fig. 1b) which was analyzed by Eqn. 1.

$$y = \frac{a + b \cdot c \cdot x^n}{1 + c \cdot x^n} \quad (1)$$

Where a and b are the absorbances in the absence and presence of excess of NO, c is the apparent formations constant of the product and n is the stoichiometry of the reaction. The evaluated parameters are: $K_f = (1.65 \pm 0.6) \times 10^4 \text{ M}^{-1}$ and $n=1.0$ (Fig. 1b).

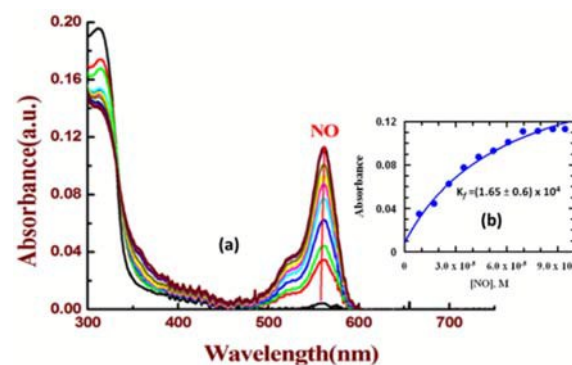


Fig. 1. (a) Changes in UV-Vis absorption spectra of L^3 ($20 \mu\text{M}$) in aqueous HEPES buffer (20 mM) at pH 7.20, $\mu = 0.05 \text{ M}$ NaCl with variable concentrations of NO ($0 - 80 \mu\text{M}$). (b) nonlinear curve fitting.

Fluorescence studies

Again, on gradual addition of NO (0–60.0 μM) to the non-fluorescent solution of L^3 (20.0 μM), a 11-fold enhancement in fluorescence intensity at 587 nm was observed on excitation at 510 nm (Fig. 2a), which also suggests an opening of the spirolactam ring of L^3 on reaction to the NO ion.²¹ A plot FI vs. [NO] gives a non linear curve, which gives $c = K_f = (7.55 \pm 2.04) \times 10^4 \text{ M}^{-1}$ (Fig. 2b). The 1:1 L^3 :NO binding was further supported by mass spectrometric analysis (m/z):530.55 [(Rh-en-ONO)](3) (Fig.S3c in the Supporting Information).

Selectivity Studies

The addition of 5 equivalents of Mn^{2+} , Fe^{3+} , Co^{2+} , Ni^{2+} , Cu^{2+} , Cr^{3+} , Zn^{2+} , Pb^{2+} , Cd^{2+} , Al^{3+} , Hg^{2+} , Na^+ , K^+ and Mg^{2+} have no influence on the fluorescence detection of NO (Fig. S5a). NO detection was not perturbed in the presence of different anions like SCN^- , NO_3^- , N_3^- , Cl^- , Br^- , F^- , HCO_3^- , ClO_4^- , H_2O_2 , OAc^- , $\text{S}_2\text{O}_3^{2-}$, CN^- etc 5 equivalents of which were added into the solution of L^3 (20 μM) (Fig. S5b).

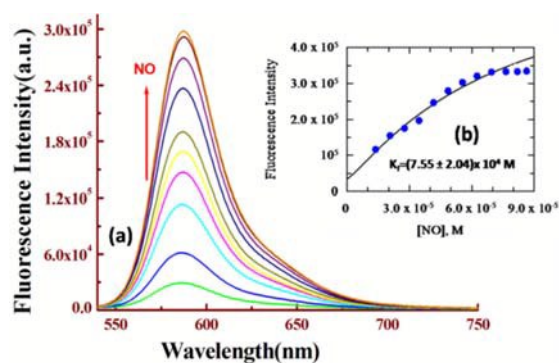


Fig. 2. (a) Changes in fluorescence spectra of L^3 (20 μM) in aqueous HEPES buffer (20 mM) at pH 7.20, $\mu = 0.05 \text{ M NaCl}$ with variable concentrations of NO (0 – 60 μM) ($\lambda_{\text{ex}} = 510 \text{ nm}$). (b) non-linear fitting.

Various types of amino acids such as phenyl alanine, valine, methionine, glutamine, isoleucine, lycine, leucine, proline, asparagine, tryptophan, hydroxyproline, aspartic acid, glutamic acid etc. do not interfere with the detection of NO by the sensor (Fig. S6). The detection of NO also remains unaffected in the presence of H_2O_2 , O_2^- , ONOO^- , TEMPO radical, OCl^- , ascorbic acid, dehydro ascorbic acid, OH^- and HNO (Fig. 3). We have also checked the selectivity of NO towards sensor L^3 over the other analogous sensor like L^4 . It was interesting to note that L^4 remains silent towards NO signifying L^3 as a selective sensor towards NO (Scheme 3). The quantum yield of L^3 -NO complex was determined to be $\Phi = 0.77$ (rhodamine 6G was used as a standard), whereas the free ligand is non or very weakly fluorescent ($\Phi = 0.07$). The limit of detection (LOD) of NO was determined by 3σ method and found to be as low as 83.4 nM (Fig. S7a). All these findings indicate that L^3 is a good example of an ideal chemosensor for NO.

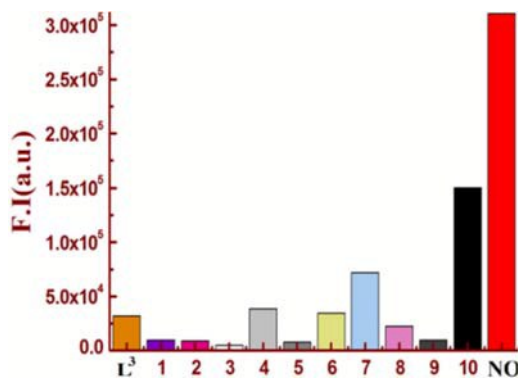


Fig. 3. Bar chart illustrating fluorescence responses of L^3 at 587 nm ($\lambda_{\text{ex}} = 510 \text{ nm}$) towards different biomolecules and anions in aqueous HEPES buffer (20 mM) at pH 7.20, $\mu = 0.05 \text{ M NaCl}$. $\text{L}^3 = 20 \mu\text{M}$. (1) H_2O_2 (2) O_2^- (3) ONOO^- (4) TEMPO radical, (5) OCl^- (6) Ascorbic Acid (7) Dehydroascorbic Acid (8) OH^- (9) HNO (10) NONOate (100 μM).



Scheme 3: Analogous Schiff base compound (L^4) with negligible fluorescence response.

pH Studies

To check the suitability for convenient biological application of this sensor towards NO sensing under physiological conditions the pH-stability of the sensor was investigated which showed no obvious fluorescence of L^3 between pH 4 and 12, suggesting the existence of spirolactam form of L^3 over this wide range of pH (Fig. 4). However, in the presence of selective guest like NO it fluoresces effectively at $\text{pH} \geq 5.0$ which clearly indicates the compatibility of the sensor for biological applications under physiological conditions.

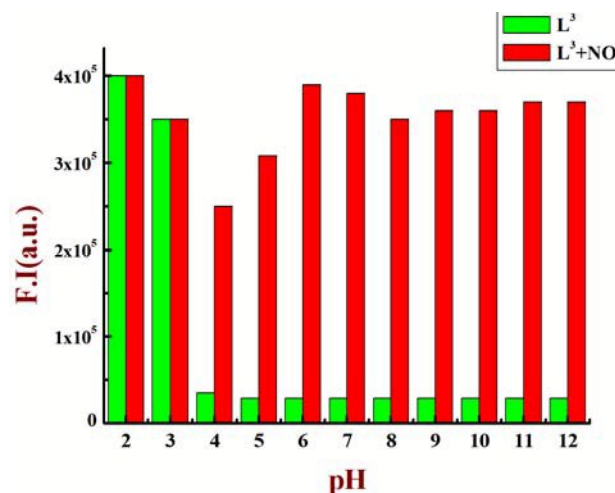


Fig. 4. pH dependent fluorescence response of L³ and in the presence of NO.

Actually this ligand behaves as a chemodosimeter to sense NO in solution. Upon addition of excess NO to the HEPES buffer solution of L³, there is a hydrolysis of the azomethyne bond with simultaneous NO induced ring opening (Fig. 5).

To establish the formation of the compound, Rh-en-ONO (**3**), by the opening of the spirolactam ring (Fig. 5), we have separated the products using column chromatography after purging NO into the solution of ligand (L³) in CH₃CN. The column was prepared with neutral alumina (Al₂O₃) by passing CH₃CN in the presence of few drops of ammonia. A slurry of the reaction mixture (after purging NO into the solution of ligand (L³)) in CH₃CN was prepared. Then CH₃CN:CH₂Cl₂=9:1 (v/v) was passed through the column to separate the products. We have characterised the isolated products by ¹H and ¹³C NMR, Mass analysis and IR studies (Fig. S1a, Fig. S1c, Fig. S2a, Fig. S2c, Fig. S3c-e, Fig. S4a and Fig. S4c).

From ¹H NMR study we can see that the reaction of L³ with NO in CH₃CN solution produces aldehyde (**1**) (Fig. S1a) with a new peak at 10.62 ppm due to the breaking of azomethyne bond.⁴⁹ Also in ¹³C NMR, a new peak at 189.53 ppm arises due to formation of aldehyde product (**1**) (Fig. S2a). Due to the formation of Rh-en-ONO product (**3**) the tertiary carbon of L³ at 64.62 ppm is completely vanished signifying NO assisted opening of the spirolactam ring (Fig. S2c). Also from the mass analysis it is confirmed that the aldehyde (**1**) and Rh-en-ONO (**3**) are formed (Fig. S3c-e).

The formation of the compound, Rh-en-ONO (**3**), by opening of the spirolactam ring (Fig. 5) was established through IR studies. The IR studies revealed that the characteristic stretching frequency of the amidic 'C=O' of the rhodamine moiety appeared at 1681 cm⁻¹. Another stretching frequency observed at 2965 cm⁻¹ corresponds to the N-H band. Peaks at 1560 and 1350 cm⁻¹ (N-O stretching frequency)⁵⁰ were observed due to bound ONO (Fig. S4c). For aldehyde product (**1**) the stretching frequency at 1690 cm⁻¹ is obtained for -CHO group. (Fig. S4a). This is further confirmed by IR

spectra obtained by DFT studies on such compound (Fig. S8 and Table S1).

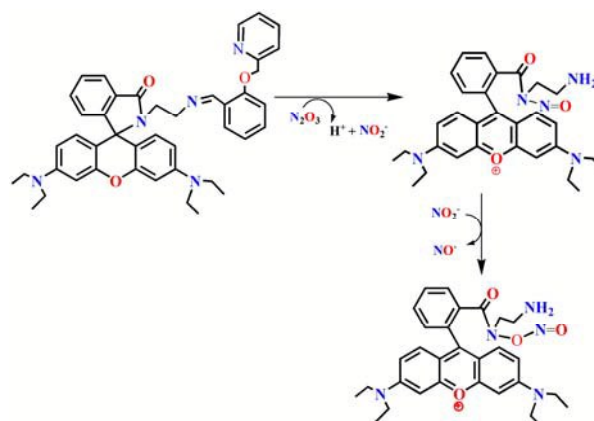


Fig. 5. Proposed reaction mechanisms of ring opening with NO.

Geometry optimization and electronic structure

In order to get some idea of the bonding mode of the ligand with NO we have carried out DFT optimization on NO-L³ compound. The optimized geometries of L³ and its ONO bound form are shown in Fig. 6. The composition of the compound NO-L³ has been adopted based on HRMS studies and found as [(Rh-en-ONO)] (**3**). L³ and [(Rh-en-ONO)] species (**3**) have C1 point group. The important optimized geometrical parameters of the compound are listed in Table S2.

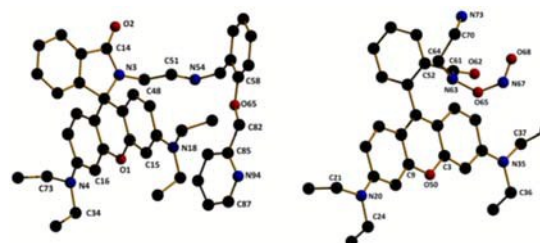


Fig. 6. Optimized structure of L³ and Rh-en-ONO compound (**3**).

In case of Rh-en-ONO compound (**3**), the calculated C61-O62 bond distance is 1.21 Å and N-O bond distances are found to fall in the range 1.17-1.29 Å. In the case of L³ in the ground state, the electron densities of the HOMO and HOMO-3 orbitals reside mainly on the chroman and xantheno moiety respectively. The energy gap between the HOMO and LUMO is 7.99 eV (Fig. 7).

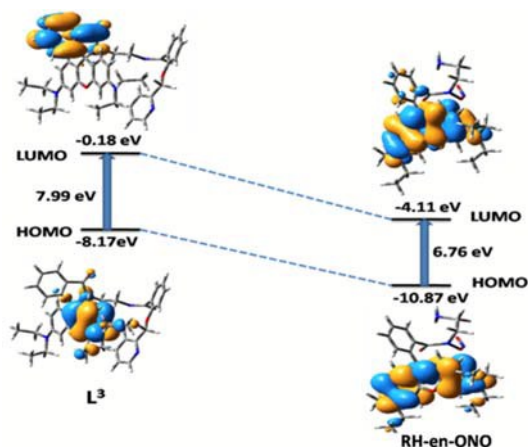


Fig. 7. Frontier molecular orbitals of L^3 and RH-en-ONO compound (**3**).

In the case of the HOMO-1 orbital in RH-en-ONO compound (**3**) the electronic contribution comes mainly from the xanthine moiety and in case of HOMO-6 it comes from the benzamine moiety. The HOMO–LUMO energy gap is 6.76 eV (Fig. 7). The UV-Vis absorption spectra of the ligand used in the present work were calculated at room temperature in H₂O by the TDDFT method. The ligand shows two well resolved peaks at 315 and 416 nm and all have ILCT character. These bands are assigned to the $S_0 \rightarrow S_{12}$ and $S_0 \rightarrow S_5$ electronic transitions, respectively (Fig. 8). The absorption energies and associated oscillator strengths are given in Table 1 and Table S3. The UV-Vis spectrum of the RH-en-ONO compound (**3**) shows three absorption bands at 476, 518 and 561 nm in H₂O at room temperature, which correspond nicely to the TDDFT calculated absorption bands located at 458.7, 500.2 and 573.9 nm. These three absorption bands can be assigned to the $S_0 \rightarrow S_{10}$, $S_0 \rightarrow S_6$ and $S_0 \rightarrow S_5$ transitions, respectively (Fig. 9) originating from ILCT transitions (Table S4).

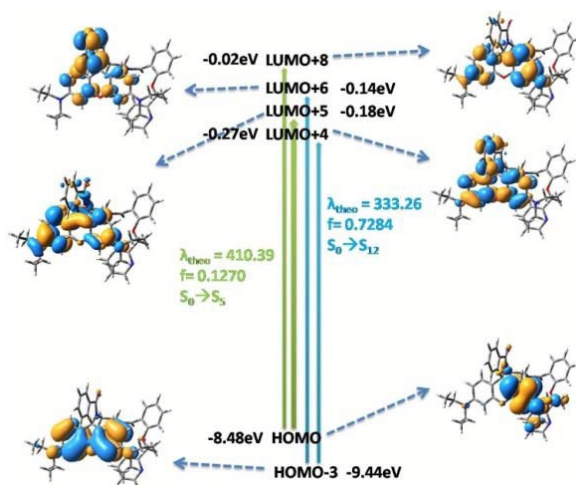


Fig. 8. Frontier molecular orbitals involved in the UV-Vis absorption of L^3 in H₂O.

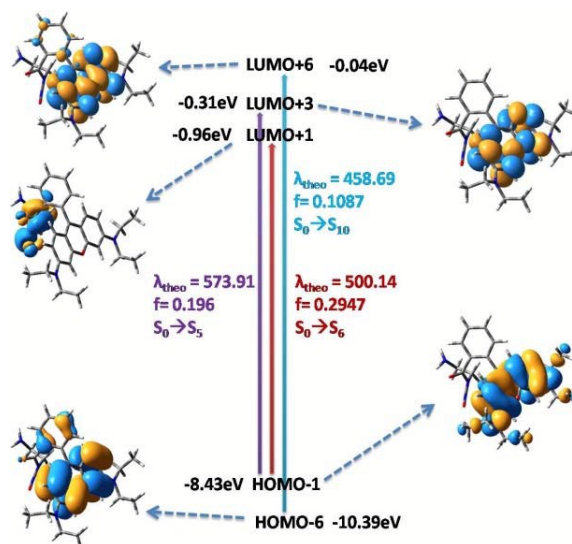


Fig. 9. Frontier molecular orbitals involved in the UV-Vis absorption of RH-en-ONO (**3**) in H₂O.

Table 1: The comparable calculated optical transitions with Experimental UV/Vis values for the ligand (L^3), RH-en-ONO compound (**3**).

Compounds	Theoretical (nm)	Experimental (nm)	Electronic Transition	f
Ligand (L^3)	333.26	315	$S_0 \rightarrow S_{12}$	0.7284
Ligand (L^3)	410.39	416	$S_0 \rightarrow S_5$	0.1270
RH-en-ONO compound (3)	573.9	561	$S_0 \rightarrow S_5$	0.196
RH-en-ONO compound (3)	500.2	518	$S_0 \rightarrow S_6$	0.2947
RH-en-ONO compound (3)	458.7	476	$S_0 \rightarrow S_{10}$	0.1087

Cell Imaging Studies.

The cytotoxicity effects of L^3 were determined by cell viability assay on HepG2 cells. Up to 60 μ M of L^3 have less than 30% cytotoxicity after 24 hours of L^3 treatment (Fig. 10). Spectrophotometric and fluorometric analyses reveal that L^3 has high selectivity and sensitivity for NO. In order to elucidate the biochemical importance of the L^3 we used HepG2 cell line. We have observed the increase in NO level after treatment of SNP or (L-Arg + LPS+IFN- γ) (S) compared to control and were mitigated followed by treatment with SMT (Fig. 11A). To confirm the iNOS mediated production of NO, we have checked the iNOS expression after treatment of SNP or (L-Arg and LPS+IFN- γ) (S) and also with SMT compared to control at mRNA and protein level (Fig. 11B-C). We have observed that increased in iNOS expression after treatment either with SNP or (L-Arg and LPS+IFN- γ)

ARTICLE

Journal Name

compared to control and were abrogated after simultaneous treatment with SMT (Fig.11A-B).

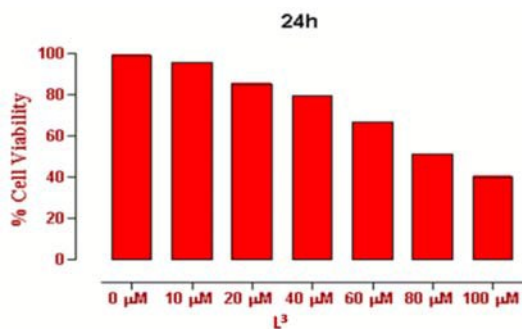


Fig.10. % Cell viability detection by using MTT assay of L³ on HepG2 cells treated for 24h.

For *in vitro* confirmation that L³ forms the complex with intracellularly produced NO, we have treated the HepG2 cells with

1μM/mL SNP and (10 μM/mL L-Arg and 0.5 μg/mL LPS+ 5ng/mL IFN-γ) to induce NO production for 24 hour followed by incubation with 10 μM/mL L³ for 30 min. Clear intracellular cytoplasmic red fluorescence signal was observed.

Fig. 11 gives the direct NO level measurement by Griess assay after NO inducer treatment along with iNOS inhibitor SMT compared to control after 24 Hour. To establish the selective and specific NO reaction of L³ HepG2 cells were co-treated with nitric oxide Synthase (NOS) inhibitor S-methylisothiourea (SMT) along with NO inducer, weak or no red signal were observed compared to that of control cells suggesting that L³ sensor selectively and specifically react with intracellularly produced NO (Fig. 12). Likely to track the *in vivo* NO sensing capability, we incubate 4-5 week old zebrafish with 20 μM of L³ for 45 min (zebrafish was alive) and shows high specific red fluorescence compared to control (Fig. 13). Overall it suggests that the novel L³ sensor is non-cytotoxic, cell permeable and suitable for both *in vitro* and *in vivo* NO sensing capability.

Journal Name

ARTICLE

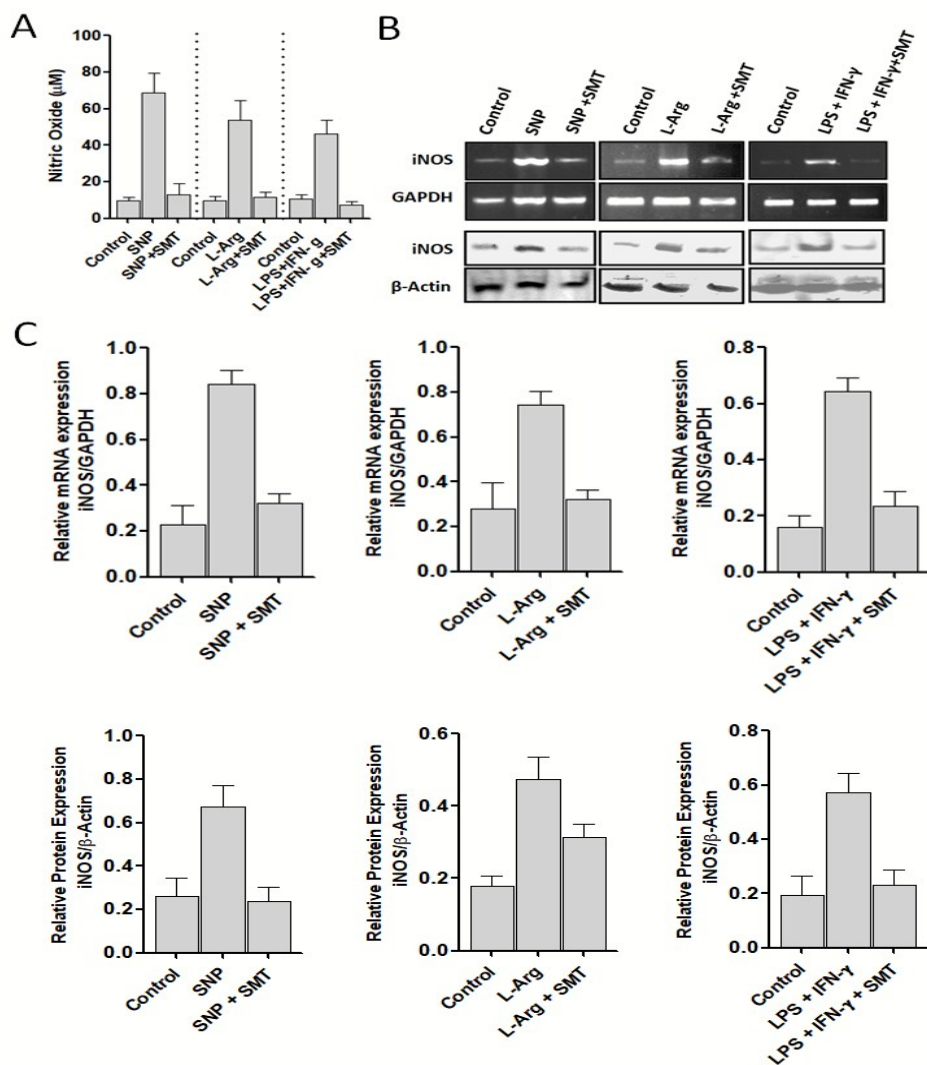


Fig. 11. (A) Graphical representation (Mean \pm SD) of direct NO level measurement by Griess assay after NO inducer treatment along with iNOS inhibitor SMT compared to control after 24 Hour. (B) iNOS level after treatment with NO inducer along with iNOS inhibitor SMT compared to control at 24 Hour by using RT-PCR and western blot analysis. GAPDH and β -actin was used as internal control. (C) Quantitative analysis and graphical representation (Mean \pm SD) of iNOS level after treatment with NO inducer along with iNOS inhibitor SMT compared to control at 24 Hour by using RT-PCR and western blot analysis.

Journal Name

ARTICLE

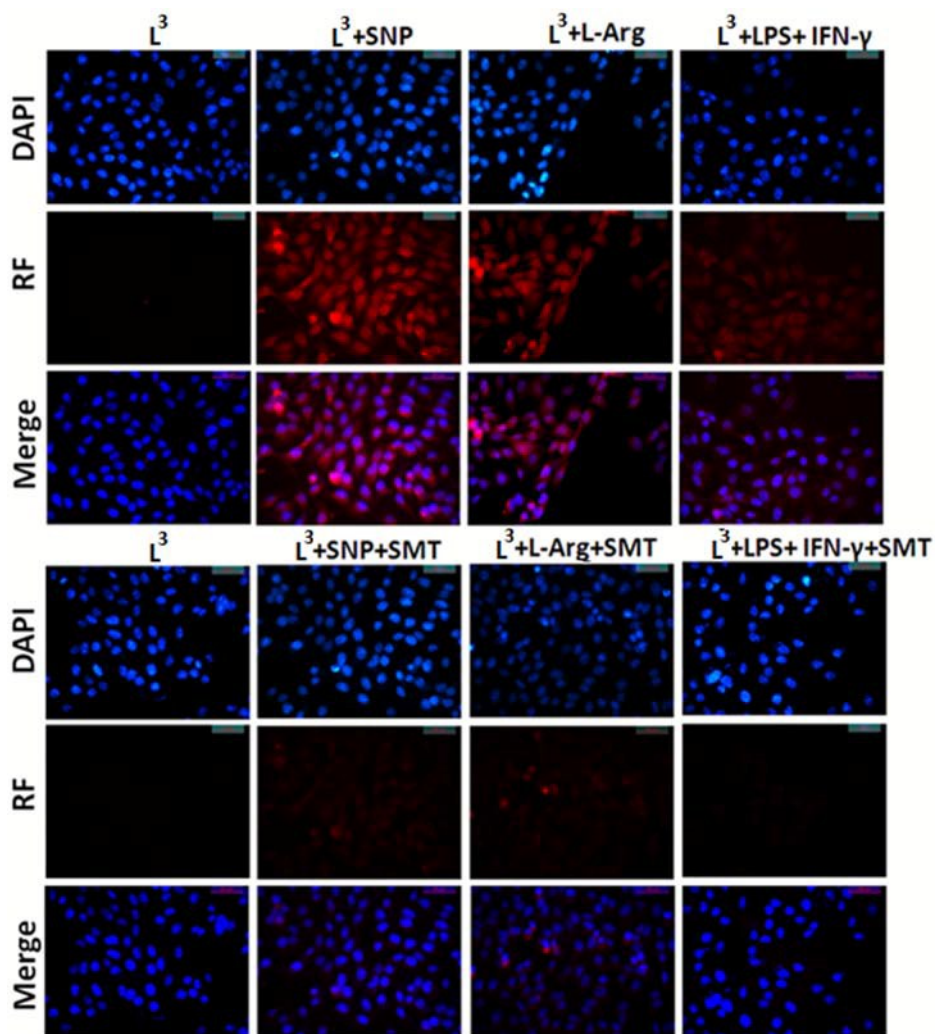


Fig. 12. The fluorescence images of HepG2 cells captured (40X) after treatment with NO inducer 1 μ M/mL SNP, (10 μ M/mL L-Arg + 0.5 μ g/mL LPS+ 5ng/mL IFN- γ) and along with iNOS inhibitor 10 μ M/mL SMT compared to control for 24 hour, the media were replaced with fresh conditioned media and treated with 10 μ M/mL L^3 for 30 min at 37°C. The image shows the strong cytoplasmic red fluorescence when L^3 complexes with intracellular NO compared control. There was weak or no red fluorescence was observed for NO inducer treated along with SMT. Cytoplasmic complex formation was confirmed by nuclear stain DAPI.

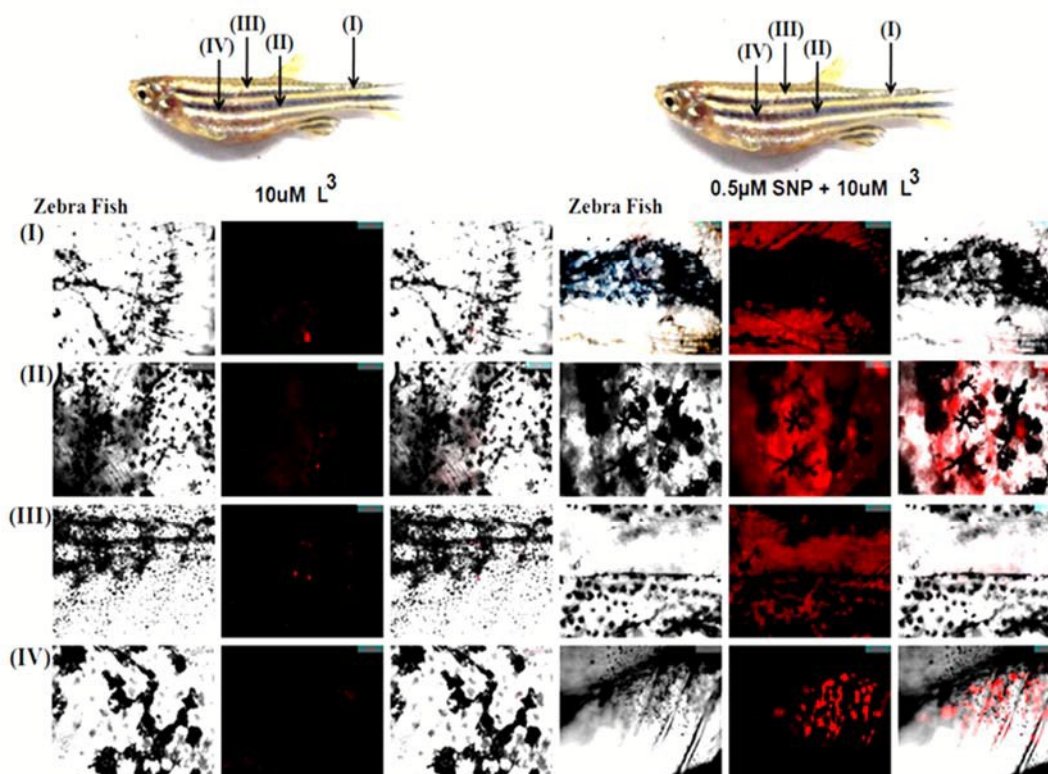


Fig. 13. The phase contrast and fluorescence images of zebrafish shows *in vivo* selective and specific NO chelating capability, 4-5 week old zebrafish incubated with 20 μ M of L^3 for 45 min and shows high specific red fluorescence compared to control (40X objective).

Conclusion

In summary, a novel Rhodamine B based dual channel sensor (L^3) has been synthesized and structurally characterized. In aqueous HEPES buffer (20 mM) at pH 7.20, $\mu = 0.05$ M NaCl it selectively recognizes NO with 11 fold fluorescence enhancement with the formation constant of $(7.55 \pm 2.04) \times 10^4 \text{ M}^{-1}$ through an unusual formation of nitrosohydroxylamine which leads to the opening of spirolactam ring. An analogous Schiff base compound (L^4) does not show any response towards NO, clearly indicating the selective response of L^3 towards NO (Scheme 3, Figs. S9, S10). Again, the addition of 5 equivalents different metal ions, anions, amino acids and various biological species do not interfere with the detection of NO. Quantum yields of L^3 and [$L^3 + \text{NO}$] compound are found to be 0.07, 0.77 respectively using Rhodamine-6G as standard. LOD for NO were determined by 3σ methods and found to be 83.4 nM. L^3 and [$L^3 + \text{NO}$] compound were optimized by DFT studies. The UV-Vis absorption spectra of the ligand and [$L^3 + \text{NO}$] showed excellent match with the result calculated by the TDDFT method at room temperature in H_2O . IR frequency of L^3 and [$L^3 + \text{NO}$] compound were found to be similar with the IR spectra obtained by DFT studies on such compound. L^3 sensor is non-cytotoxic, cell permeable and suitable for both *in vitro* and *in vivo* NO sensing capability.

Acknowledgement

Financial support from the Department of Science and Technology (DST), Government of India, New Delhi (SR/S1/IC-20/2012) and DST (Ref. No. 809(Sanc)/ST/P/S&T/4G-9/2104) West Bengal India are gratefully acknowledged.

References

- (a) A. R. Butler and D. L. H. Williams, *Chem. Soc. Rev.*, 1993, **22**, 233; (b) B. G. Hill, B. P. Dranka, S. M. Bailey, J. R. Lancaster and V. M. Darley-Usmar, *J. Biol. Chem.*, 2010, **285**, 19699.
- J. M. Zimmet and J. M. Hare, *Circulation*, 2006, **114**, 1531.
- A. Wink, Y. Vodovotz, J. Laval, F. D. Laval and M. W. J. B. Mitchell, *Carcinogenesis*, 1998, **19**, 711.
- B. Mayer, *Nitric Oxide*, Springer, Berlin, 2000.
- L. J. Ignarro, *Nitric Oxide Biology and Pathobiology*, Academic Press, San Diego, CA, 2000.
- G. Hummel, A. J. Fisher, S. Martin, F. Q. Schafer and G. R. Buettner, *Free Radical Biol. Med.*, 2006, **40**, 501.
- (a) W. Xu, L. Z. Liu, M. Loizidou, M. Ahmed and I. G. Charles, *Cell Res.*, 2002, **12**, 311; (b) B. Mitrovic, L. J. Ignarro, H. V. Vinters, M. A. Akers, I. Schmid and C. Uittenbogaart, *Neuroscience*, 1995, **65**, 531; (c) Y. Hou, J. Wang, P. R. Andreana, G. Cantauria, S. Tarasia, L. Sharp, P.

ARTICLE

Journal Name

- G. Braunschweiger and P. G. Wang, *Bioorg. Med. Chem. Lett.*, 1999, **9**, 2255.
- 8 E. M. Hetrick and M. H. Schoenfisch, *Annu. Rev. Anal. Chem.*, 2009, **2**, 409.
- 9 H. Kojima, N. Nakatsubo, K. Kikuchi, S. Kawahara, Y. Kirino, H. Nagoshi, Y. Hirata and T. Nagano, *Anal. Chem.*, 1998, **70**, 2446.
- 10 A. Dejam, C. J. Hunter, C. Tremonti, R. M. Pluta, Y. Y. Hon, G. Grimes, K. Partovi, M. M. Pelletier, E. H. Oldfield, R. O. Cannon, A. N. Schechter and M. T. Gladwin, *Circulation*, 2007, **116**, 1821.
- 11 D. A. Wink, J. F. Darbyshire, R. W. Nims, J. E. Saavedra and P. C. Ford, *Chem. Res. Toxicol.*, 1993, **6**, 23.
- 12 D. J. Stuehr and M. A. Marletta, *Proc. Natl. Acad. Sci. USA* 1985, **82**, 7738.
- 13 P. Heiduschka and S. Thanos, *NeuroReport*, 1998, **9**, 4051.
- 14 P. Meineke, U. Rauen, H. de Groot, H. -G. Korth and R. Sustmann, *Chem. Eur. J.*, 1999, **5**, 1738.
- 15 H. Kojima, M. Hirotoni, N. Nakatsubo, K. Kikuchi, Y. Urano, T. Higuchi, Y. Hirata and T. Nagano, *Anal. Chem.*, 2001, **73**, 1967.
- 16 Y. Gabe, Y. Urano, K. Kikuchi, H. Kojima and T. Nagano, *J. Am. Chem. Soc.*, 2004, **126**, 3357.
- 17 E. Sasaki, H. Kojima, H. Nishimatsu, Y. Urano, K. Kikuchi, Y. Hirata and T. Nagano, *J. Am. Chem. Soc.*, 2005, **127**, 3684.
- 18 M. H. Lim, D. Xu and S. J. Lippard, *Nat. Chem. Biol.*, 2006, **2**, 375.
- 19 G. Sivaraman, T. Anand and D. Chellappa, *ChemPlusChem.*, 2014, **79**, 1761.
- 20 H. Zheng, G. -Q. Shang, S. -Y. Yang, X. Gao and J. -G. Xu, *Org. Lett.*, 2008, **10**, 2357.
- 21 H. Kojima, M. Hirotoni, N. Nakatsubo, K. Kikuchi, Y. Urano, T. Higuchi, Y. Hirata and T. Nagano, *Anal. Chem.*, 2001, **73**, 1967.
- 22 X. Hu, J. Wang, X. Zhu, D. Dong, X. Zhang, S. Wu and C. A. Duan, *Chem. Commun.*, 2011, **47**, 11507.
- 23 R. Alam, T. Mistri, P. Mondal, D. Das, S. K. Mandal, A. R. Khuda-Bukhsh and M. Ali, *Dalton Trans.*, 2014, **43**, 2566.
- 24 W. Hu, D. Boateng, J. Kong and X. Zhang, *Austin J. Biosens. Bioelectron.*, 2015, **1**, 1.
- 25 Y. Gabe, Y. Urano, K. Kikuchi, H. Kojima and T. Nagano, *J. Am. Chem. Soc.*, 2004, **126**, 3357.
- 26 E. Sasaki, H. Kojima, H. Nishimatsu, Y. Urano, K. Kikuchi, Y. Hirata and T. Nagano, *J. Am. Chem. Soc.*, 2005, **127**, 3684.
- 27 Y. Yang, S. K. Seidlits, M. M. Adams, V. M. Lynch, C. E. Schmidt, E. V. Anslyn and J. B. Shear, *J. Am. Chem. Soc.*, 2010, **132**, 13114.
- 28 L. E. McQuade, M. D. Pluth and S. J. Lippard, *Inorg. Chem.*, 2010, **49**, 8025.
- 29 L. E. McQuade and S. J. Lippard, *Inorg. Chem.*, 2010, **49**, 7464.
- 30 M. H. Lim and S. J. Lippard, *Inorg. Chem.*, 2004, **43**, 6366.
- 31 H. Li and A. Wan, *Analyst*, 2015, **140**, 7129.
- 32 A. Beltran, M. Isabel Burguete, D. R. Abánades, S. D. Perez-Sala, V. Luis and F. Galindo, *Chem. Commun.*, 2014, **50**, 3579.
- 33 M. H. Lim and S. J. Lippard, *J. Am. Chem. Soc.*, 2005, **127**, 12170.
- 34 M. H. Lim and S. J. Lippard, *Inorg. Chem.*, 2006, **45**, 8980.
- 35 C. Sun, W. Shi, Y. Song, W. Chen and H. Ma, *Chem. Commun.*, 2011, **47**, 8638.
- 36 A. S. M. Islam, R. Bhowmick, K. Pal, A. Katarkar, K. Chaudhuri, and M. Ali, *Inorg. Chem.*, 2017, **56**, 4324.
- 37 T. -W. Shiue, Y. -H. Chen, C. -M. Wu, G. Singh, H. -Y. Chen, C. -H. Hung, W. -F. Liaw and Y. -M. Wang, *Inorg. Chem.*, 2012, **51**, 5400.
- 38 F. -H. Wanga, C. -W. Chenga, L. -C. Duana, W. Lei, M. -Z. Xia and F. -Y. Wang, *Sensors and Actuators B*, 2015, **206**, 679.
- 39 M. J. Frisch, et. al. GAUSSIAN 09 (Revision A.1), Gaussian, Inc., Wallingford, CT, 2009.
- 40 M. E. Casida, C. Jamoroski, K. C. Casida and D. R. Salahub, *J. Chem. Phys.*, 1998, **108**, 4439.
- 41 R. E. Stratmann, G. E. Scuseria and M. J. Frisch, *J. Chem. Phys.*, 1998, **109**, 8218.
- 42 V. Barone and M. Cossi, *J. Phys. Chem.*, 1998, **102**, 1995.
- 43 M. Cossi and V. Barone, *J. Chem. Phys.*, 2001, **115**, 4708.
- 44 M. Cossi, N. Rega, G. Scalmani and V. Barone, *J. Comput. Chem.*, 2003, **24**, 669.
- 45 A. S. M. Islam, R. Bhowmick, H. Mohammad, A. Katarkar, K. Chaudhuri and M. Ali, *New J. Chem.*, 2016, **40**, 4710.
- 46 C. Chakraborty, C. H. Hsu, Z. H. Wen, C. S. Lin and G. Agoramorthy, *Curr Drug Metab.*, 2009, **10**, 116.
- 47 A. Holmberg, C. Olsson and S. Holmgren, *J. Exp. Biol.*, 2006, **209**, 2472.
- 48 C. S. Porteus, J. Pollack, V. Tzaneva, R. W. M. Kwong, Y. Kumai, S. J. Abdallah, G. Zacccone, E. R. Lauriano, W. K. Milsom and S. F. Perry, *Journal of Experimental Biology*, 2015, **218**, 3746.
- 49 T. Mistri, R. Alam, M. Dolai, S. K. Mandal, P. Guha, A. R. Khuda-Bukhsh and M. Ali, *Eur. J. Inorg. Chem.*, 2013, 5854.
- 50 M. P. S. Andersen, M. D. Hurley, J. C. Ball, W. F. Schneider, T. J. Wallington and O. J. Nielsen, *International Journal of Chemical Kinetics*, 2003, **35**, 159.

Rhodamine-based turn-on nitric oxide sensor in aqueous medium with endogenous cell imaging: an unusual formation of nitrosohydroxylamine

Rabiul Alam^a, Abu Saleh Musha Islam^a, Mihir Sasmal^a, Atul Katarkar^b and Mohammad Ali^{a,*}

A sensor (**L**³) has been developed for highly sensitive and selective recognition for NO in purely aqueous medium with an unusual formation of nitrosohydroxylamine leading to selective opening of spirolactam ring with prominent enhancement in emission intensities and *in vivo* NO sensing in Zebra fish was also checked.

